Preparation of Oil Shale Ash Filled High Density Polyethylene Composite Materials and their Characterization

RAID BANAT[*1], MANAL AL-RAWASHDEH[1] AND HEBA ALKHLAIFAT[1]

[*1]Department of Chemistry, Al al-Bayt University, P.O. BOX 130040, Mafraq, 25113, Jordan.

ABSTRACT

Composite of oil Shale ash (OSA) filler and high density polyethylene (HDPE) matrix was formulated and studied. OSA mainly composed of Ca, Si, and Fe most of which in oxide forms. OSA-HDPE composite with 0, 5, 10, 15, 20, and 25 wt. % OSA were produced using extrusion and hot press. Mechanical, morphological, and water uptake properties of the composite are discussed herein. While the tensile stress at yield, 47 MPa, restored its value close to the neat HDPE, an increase in the mean values of the tensile stress at rapture from 19 to 33 MPa, the tensile modulus from 250 to 350 MPa, the flexural strength from 17 to 22 MPa, and the flexural modulus from 1.8 to 2.4 GPa was obtained upon increasing the OSA content. However, the decrease in the mean values of the tensile strain at yield, from 34 to 27 % (for higher OSA load), the tensile stain at rapture from 160 to 40 %, and the impact strength from 65 to 50 MPa were observed upon increasing the OSA content. Water uptake was marginally increased, from 0.35 to 0.50%, with the filler loading. OSA-HDPE composite apparently remained stiff and hard with almost no deformation due to water contact. Microstructures obtained from scanning electron microscopy were in good agreement with the apparent mechanical performance. OSA-HDPE composite have superior properties compared to the neat HDPE.

KEYWORDS: *Oil shale ash, HDPE, Composite, Mechanical properties.*

1. INTRODUCTION

Oil shale reserve is considered as a very important substituent for petroleum. Oil shales are fine-grained rocks, contain organic material that can be refined into fuels.[1] Organic matter (15%–55%), calcite (>50%), dolomite (10%–15%), and siliciclastic minerals (10–15%) are the main constituents of oil shale. Geologic

studies have shown that Jordan contains several oil shale deposits with good quality and rich in organic matter at shallow depth. Jordanian oil shale with relatively low ash and moisture contents have a gross calorific value of 7.5 MJ/kg, and an oil yield of 8 to 12%.[2] Jordan together with international companies and partners have leading and executing a power project that harvesting energy since mid of 2020. Developing a 554 MW oil shale fired power plant in Jordan is considered as the most advanced development project outside Estonia, one of the world leaders in oil shale industry.[3] Combustion of oil shale in thermal power plants at high temperatures as high as 1500°C resulted in harvesting energy and producing by product wastes. Research on reducing hazardous effect, of wastes from oil shale combustion process, on environment has gained momentum in recent years.[4,5] Oil shale fly ash (OSFA) is a potentially hazardous material to aquatic organisms. High alkalinity of the OSFA leachates (pH>10) is apparently a serious threat to environment.[6] Storing of highly alkaline waste (OSA) material resulted from oil shale processing is a serious environmental problem.[7] A potential sustainable solution for reducing OSFA wastes and converting it into a value-added product was investigated by Zhang Z. et al., where OSFA based glass-ceramic material was produced via melting process.[8] In recent years researches on utilization of eco-friendly fly ashes have developed yet advances to new application areas are promising. Estonia processing about 80% of oil shale worldwide, annually only 5% of OSA wastes is being utilized as an alternative raw material. OSA wastes are mainly used in construction materials,[9] Portland cement, brick manufacturing, zeolite synthesis, asphalts, [10-14] agriculture,[15] and as an adsorbent material.[16] Inventions include polymeric[17-20] mineral composite materials [21-23] and product made from Polyvinylchloride (PVC) filled oil shale ash has been filed. Oil shale ash added to the PVC contains free CaO which neutralize/ bind the HCl emitting during thermal processing of PVC and reduces the HCl emission at high temperature processing.[24] OSA waste as a filler material in polymer still partially covered in literature. In plastic industry further in depth detailed investigation using various commodity plastic and OSA formulations would shed more light on potential applications. Any advances in developing OSA - polymer composite formulations would contribute positively to economy and environment.[25-27] Most research on the OSA filled polymer composites is patented work. Little information is available in literature utilizing the OSA in polymer composites.[28] However, utilizing the OSA waste in asphalt, concrete,[29] and geo-polymers [30,31] were fairly investigated. Patented polymer composites of burnet oil shale ash up to 90%, with modified material properties and reduced price, were produced.[18] In the present study, OSA waste resulted as a by-product of oil shale combustion process has been utilized as a filler in HDPE polymer. Produced OSA-HDPE polymer composite was tested and characterized accordingly. Tensile, flexural, and impact strength, water uptake %, and surface microstructure results were discussed and investigated herein.

2. EXPERIMENTAL

2.1 Materials

The composites were formulated using HDPE (Exxon Mobil HDPE HMA 018) as polymer matrix. HDPE with melt flow index of 30 g/10 min (according to ASTM D1238 standard) was used to facilitate the composite processability. Oil shale rocks were obtained from Attarat region in Jordan and used after certain processing and conditioning as a filler material.

2.2 Methods

2.2.1 OSA Preparation

Oil shale (OS) deposit obtained from local mining region in Attarat/Jordan was subjected to crushing and grinded using Pulverisette 9 vibrating cub mill (Fristch, Germany). After which sieving was carried out for oil shale to get only fine powder sample under 65 microns. OS powder was incinerated in a muffle furnace at 600°C for 2 hours. The remaining oil shale ash (OSA) powder was sieved and kept in desiccator for further use. OSA obtained from combustion of oil shale deposit was used in this study as a filler

2.2.2 Bulk Density

Bulk density of OSA was measured by using standard method, high precision graduated cylinder was used to measure the volume of 50 g OSA after drying at 80°C for 24 hr.

2.2.3 Moisture Content

OSA powder sample with mesh size under 65 microns was placed in the aluminum dish and was weighted using digital balance (~10 g). OSA sample then placed in drying furnace and kept at 103 ± 2°C for 48 h. The moisture content was measured using equation (1)

Moisture content (%) = $[(Wt._w - Wt._o)/Wt._o]$ x 100   (1)

Where; $Wt._w$ and $Wt._o$ stand for the weight of the wet and oven dry specimen respectively.

2.2.4 XRD, XRF, and SEM

In order to evaluate microstructure morphology, chemical composition, and mineral composition properties of the OSA, samples from the OSA were subjected to the following set of analyses: microstructure using scanning electron microscopy (SEM), chemical composition using the X-ray fluorescence method (XRF) and mineral composition using of the X-ray diffraction (XRD) method.

XRD and XRF were recorded using Philips X'Pert PW 3060, operated at 45 kV and 40 mA. The fractured surface morphology of the samples was examined using Quanta 600 SEM scanning electron microscope.

2.2.5 Composite Processing

HDPE and OSA were mixed and processed by using a parallel co-rotating twin screw extruder (TSE 20, L/D: 40:1, diameter 22 mm, 8 × 78 mm2 flat die) with 7 heating zones (temperature profile: 160°C/180°C/180 °C/175°C /175°C /180°C /180°C). Screw speed rate was 50 rpm and the feed rate was 1.5 kg/h.

Extruded OSA-HDPE was then press molded using digital hot (XH-406B) press machine at 160°C. The press molding time was fixed at 20s. Composites with the OSA filler content varied from 0% to 25% were

TABLE 1. Formulation of the OSA-HDPE composites

Specimen ID	OSA (Weight %)	HDPE (Weight %)
Neat HDPE	0	100
5 % OSA-HDPE	5	95
10 % OSA-HDPE	10	90
15 % OSA-HDPE	15	85
20 % OSA-HDPE	20	80
25 % OSA-HDPE	25	75

prepared. The weight percentage of the OSA filler content in composite material was summarized in Table 1. Stainless steel molds were used to manufacture sample sheets in a press-molding machine (XH-406B). OSA-HDPE composite with pre-determined formulation was press molded in sheet form of (L: 30 x W: 20x T: 2 mm) dimensions. Standard dumbbell and rectangular shaped specimens were obtained from OSA-HDPE composite sheet. Tensile and flexural tests in accordance with ASTM standards were carried for both aforementioned shapes, respectively. Specimens of impact energy test were molded in aluminum mold with (L: 63.5±2, W: 6.4±0.2 T: 12.7±0.2 mm) standard dimensions.

3. RESULTS AND DISCUSSION

OS sample after incineration underwent 55 % weight loss due to organic matter, the remaining waste (OSA) contains a large proportion of the mineral matter. X-ray diffraction (XRD) data related to the mineral composition of the OSA is shown in **Figure 1** and summarized in **Table 2.**
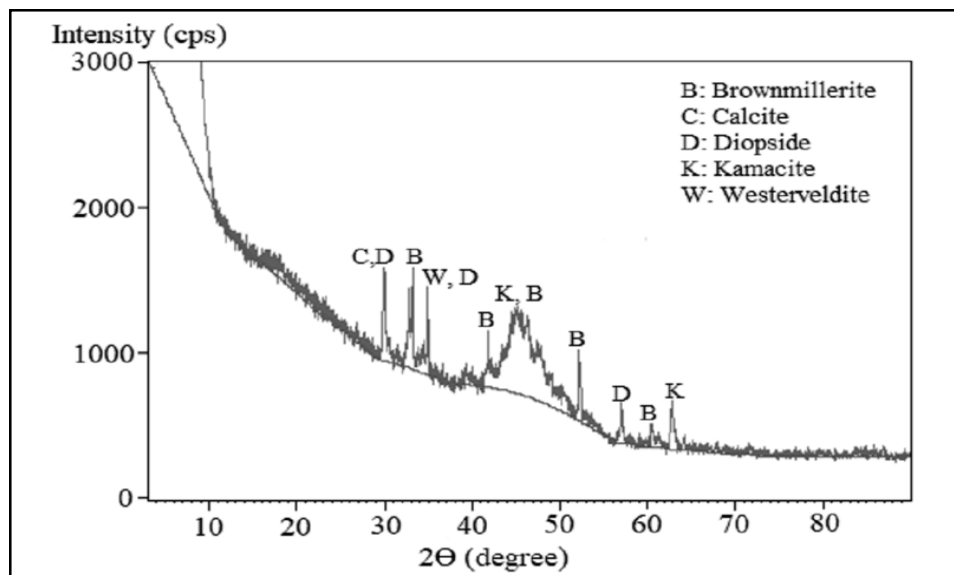

Figure 1. X-ray diffraction patterns of the oil shale ash.

XRD analysis was carried out, to determine the crystalline phases present in the OSA sample. We observed the existence of magnesium rich calcite, diopside, aluminian, silicate and brown millerite.

The X-ray fluorescence (XRF) data related to the composition of the OSA is presented in **Table 3** and **Table 4**. Results showed that the major component of the OSA is calcium, silicon and iron.

OSA samples were mainly consisted CaO, SiO_2, Al_2O_3, and Fe_2O_3. The composition of the OSA sample owing to the characteristics of the raw oil shale and the thermochemical conversions during burning process. Usta MC et al. attributed the high content of CaO to the decomposition of $CaCO_3$ which exists in the oil shale ore.[32]

TABLE 2. Mineral composition of the OSA identified by means of the XRD

(2θ)° Position	Compound Name	Notation	Chemical Formula
30	Calcite, magnesian	C	$(Ca, Mg) CO_3$
	Diopside, aluminian	D	$Ca (Mg , Al) (Si , Al)_2 O_6$
33, 33.5	Brownmillerite	B	$Ca_4 Al_2 Fe_2 O_{10}$
35	Westerveldite,	W	$(Fe, Ni, Co) As$
	Diopside, aluminian	D	$Ca (Mg , Al) (Si , Al)_2 O_6$
42	Brownmillerite	B	$Ca_4 Al_2 Fe_2 O_{10}$
45	Kamacite	K	Fe Ni
	Brownmillerite	B	$Ca_4 Al_2 Fe_2 O_{10}$
46	Kamacite	K	Fe Ni
48	Brownmillerite,	B	$Ca_4 Al_2 Fe_2 O_{10}$
52	Brownmillerite	B	$Ca_4 Al_2 Fe_2 O_{10}$
57	Diopside, aluminian	D	$Ca (Mg , Al) (Si , Al)_2 O_6$
60.5	Brownmillerite	B	$Ca_4 Al_2 Fe_2 O_{10}$
63	Kamacite	K	Fe Ni

TABLE 3. Chemical composition of the OSA oxides determined by XRF.

Oxide formula	Fe_2O_3	MnO	TiO_2	P_2O_5	SiO_2	Al_2O_3	MgO	Na_2O	CaO	K_2O
%	5.051	0.079	0.919	0.262	20.73	7.475	2.409	1.238	52.01	0.595

TABLE 4. Chemical composition of the OSA oxides determined by XRF

Element	Fe	Mn	Ti	Ca	K	P	Si	Al	Mg	Na
Intensity (kcps)	122.65	1.6425	3.8593	391.09	6.0896	2.1763	387.44	28.665	10.531	1.6011

Oil shale ashes with particle size below 65 micron have the moisture content less than 1% and the bulk density of 0.945 g/cm³ of grey color.
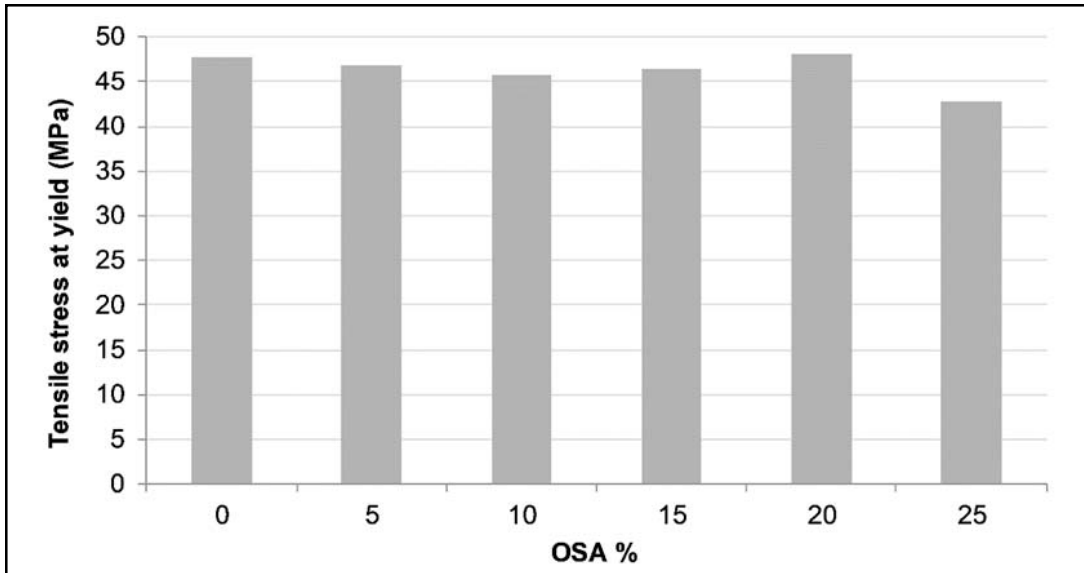
3.1 Mechanical Characterization of the OSA-HDPE Polymer Composites

3.1.1 Tensile Stress and Strain

Tensile stress of the OSA (0, 5, 10, 15, 20, and 25%) filled HDPE polymer composite is presented in **Figure 2**. The average value of five standard specimens was measured for each composite type. The tensile stress at yield for 5, 10, 15 and 20 % OSA formulations restored the same values compared to the neat HDPE. Tensile stress at yield for higher filler loading level 25% OSA decreased by 10%. The dispersion of relatively high OSA filler (25%) content in HDPE matrix may led to the polymer phase discontinuity, which decreased the elastic deformation region of the composite material compared to that of the neat HDPE

polymer. However, the OSA filler related morphological characteristics, granule size and shape are considered to play a rule in the determined mechanical performance.

2. Tensile stress at yield of the OSA-HDPE composite as a function of the filler loading.
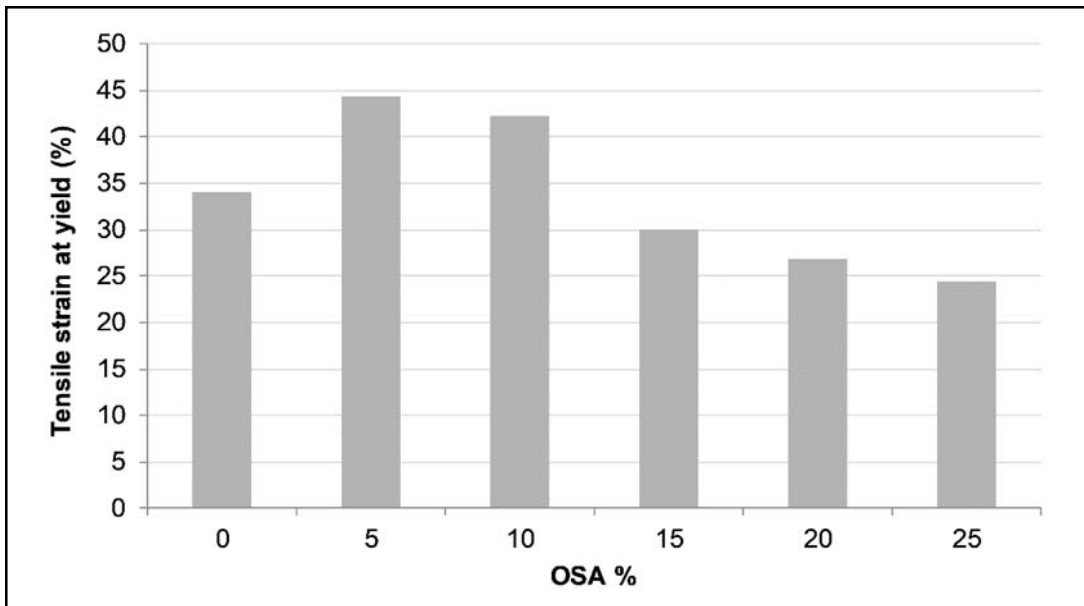

Figure 3. Tensile strain at yield of the OSA-HDPE composite as a function of the filler loading.

Moderate increase in the tensile strain at yield by 30 and 24 % as the filler content increased from 5 % to 10 % was observed **Figure 3**. On the other hand, as the filler content increased by 15, 20, and 25 % the tensile stain at yield decreased by 13, 20, and 26 % respectively, compared to the value of the neat HDPE. The elastic deformation was enhanced by the addition of small OSA quantiles 5 % and 10 % seems not to affect the matrix phase discontinuity due to the addition of well dispersed fine OSA particulate. However, increasing the OSA loading level, above 15 %, led to the decline in the elastic range of the composite specimens due to the reduction in the polymer phase extensibility.
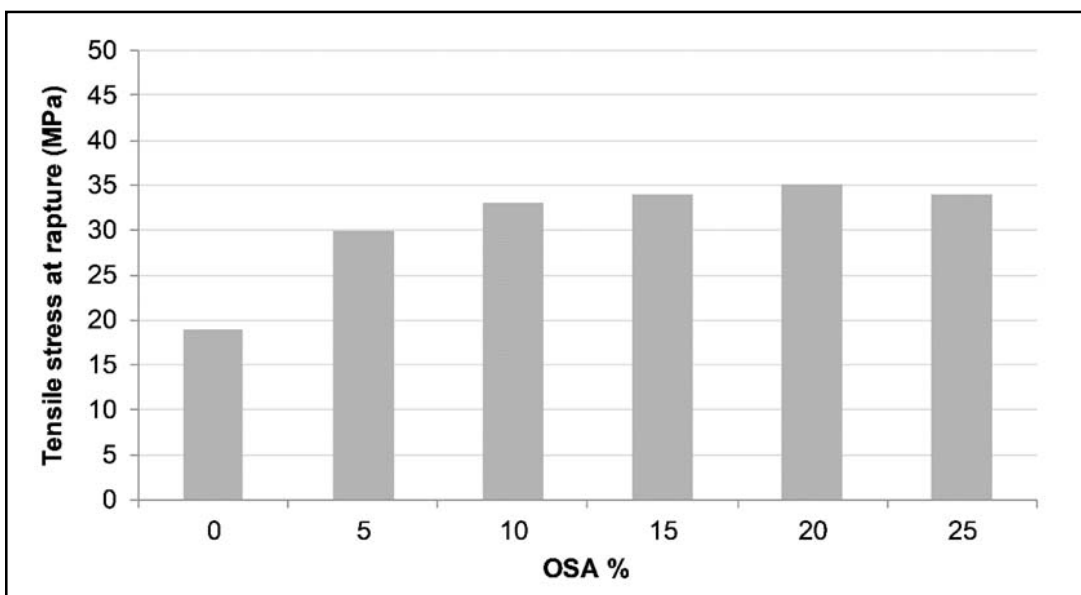

Figure 4. Tensile stress at rapture of the OSA-HDPE composite as a function of the filler loading.

Tensile stress at rapture increased by an average value of 70 % upon increasing the filler content from 5 to 25% compared to the neat HDPE value **Figure 4**. Whereas the tensile strain at rapture decreased by an average value of 50 to 80% upon increasing the filler content from 5 to 25% compared to the neat HDPE value **Figure 5**. The OSA filler decreased the extensibility and the softness of the polymer composite due to the good interfacial interaction between the binary filler matrix phases. The present findings were in good agreement with the previously published work by Leong YW et al. who studied the mechanical properties of talc filled polypropylene composite specifically the interfacial interaction between the filler and the polymer. They found that the increase in tensile strength was attributed to the good filler–polymer interactions which may resulted fromthe wettability of the OSA by the polymer matrix. Moreover, fewer micro-voids present between the fillers and matrix would assisted the stress transfer from the matrix to the fillers during external loading.[33]
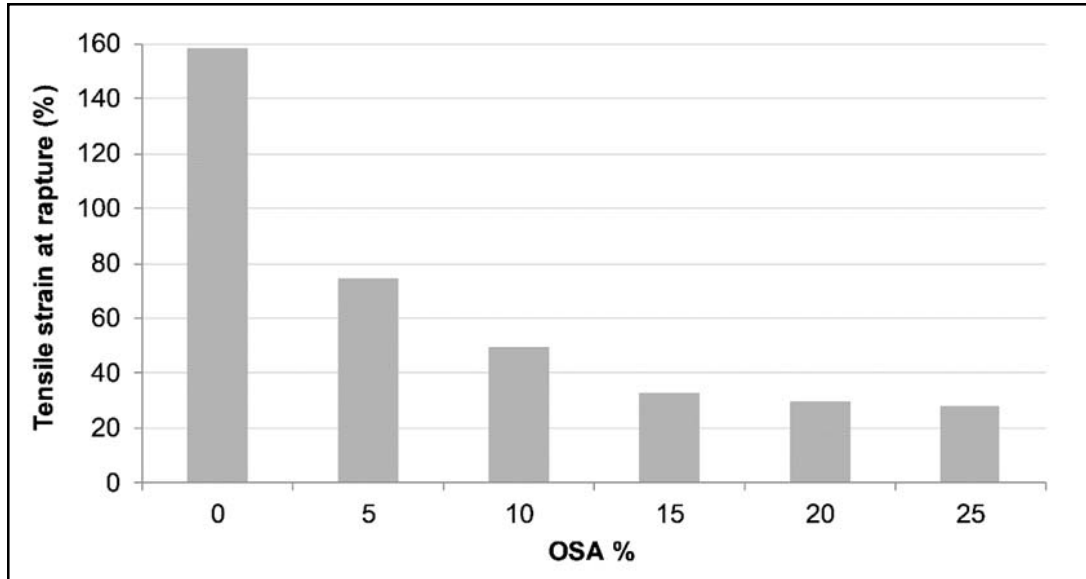
Fig. 5. Tensile strain at rapture of the OSA-HDPE composite as a function of the filler loading.

3.1.2 Modulus of Elasticity

Tensile Modulus of the OSA-HDPE was measured in the tensile test. The change in the tensile modulus as a function of the OSA filler content is shown in **Figure 6**. Tensile modulus increased with the increase of OSA loading level and reached 75% for 25% OSA specimen compared to the neat HDPE polymer. This is consistent with the values obtained for the tensile stress and the tensile strain at yield in the earlier figures. Addition of 5% to 25% OSA filler to the polymer composite apparently produced composite with a compatible mechanical performance. Filler dispersion and interfacial adhesion parameters seemed to play an active role in the resulted mechanical performance. The present findings were supported by an earlier study carried by Pukanszky et al.[34] where small stresses are generated by applying small values of strain.

Such small stresses are not enough to rapture the weak interfacial interactions. Hence, the small stresses can be transferred from polymer matrix to the OSA filler therefore allowing the filler to donate its high modulus to the composite material.

3.1.3 Flexural Strength and Modulus

Flexural properties of the OSA-HDPE composite were evaluated in the present work. Inclusion of the OSA to HDPE improved the flexural strength and modulus. Small particle size under 65 microns would have better surface area of interaction between the filler and the polymer as a result the composite stiffness is significantly improved.

Flexural strength and modulus values of the OSA filled composites at varying percentages of the OSA are shown in **Figure 7** and **8,** respectively. It was noticed that flexural strength
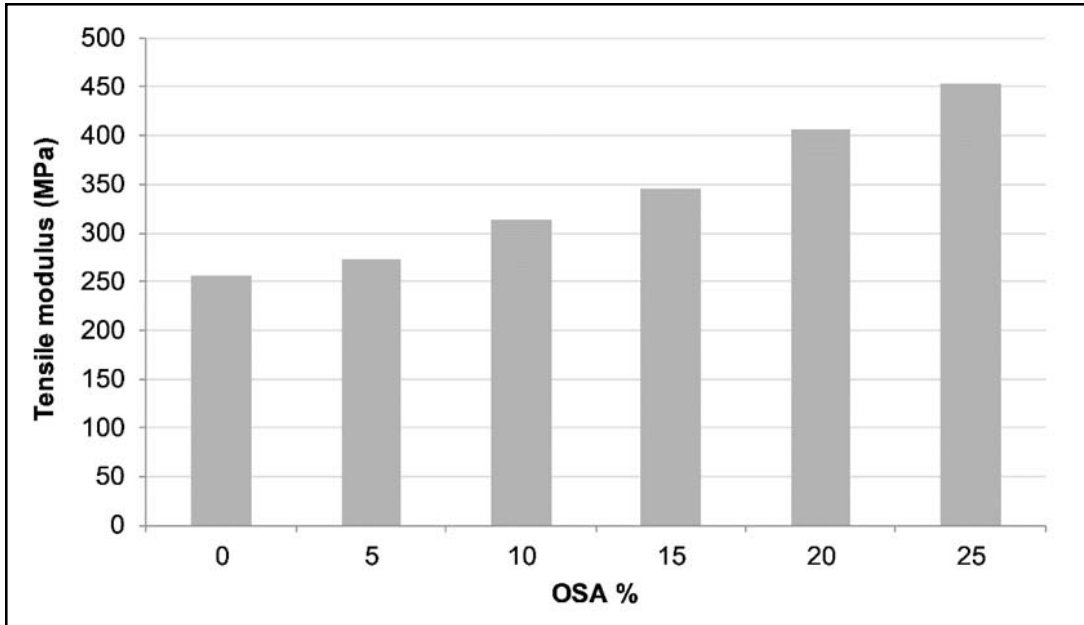
Figure 6. Tensile modulus of the OSA-HDPE composite as a function of the filler loading.
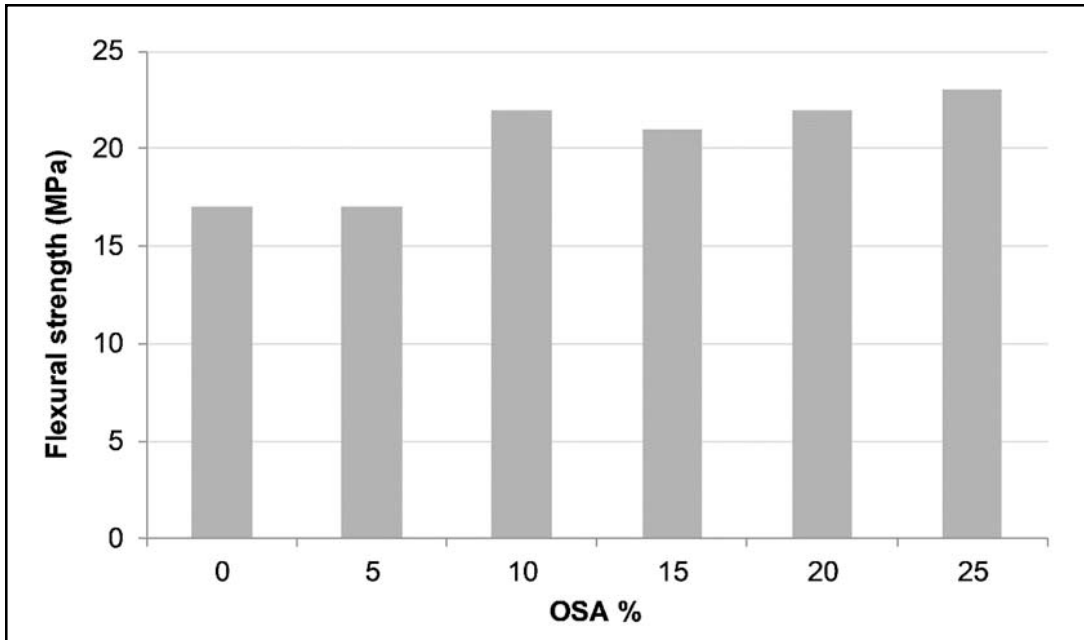

Figure 7. Flexural strength of the OSA-HDPE composite as a function of the filler loading.
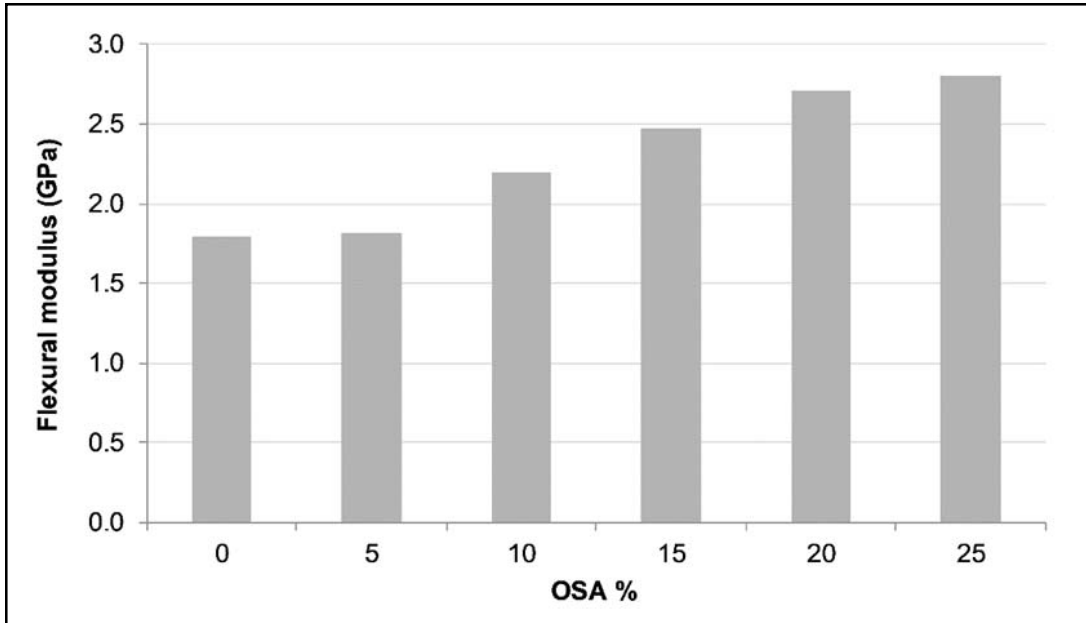
Figure 8. Flexural modulus of the OSA-HDPE composite as a function of the filler loading.
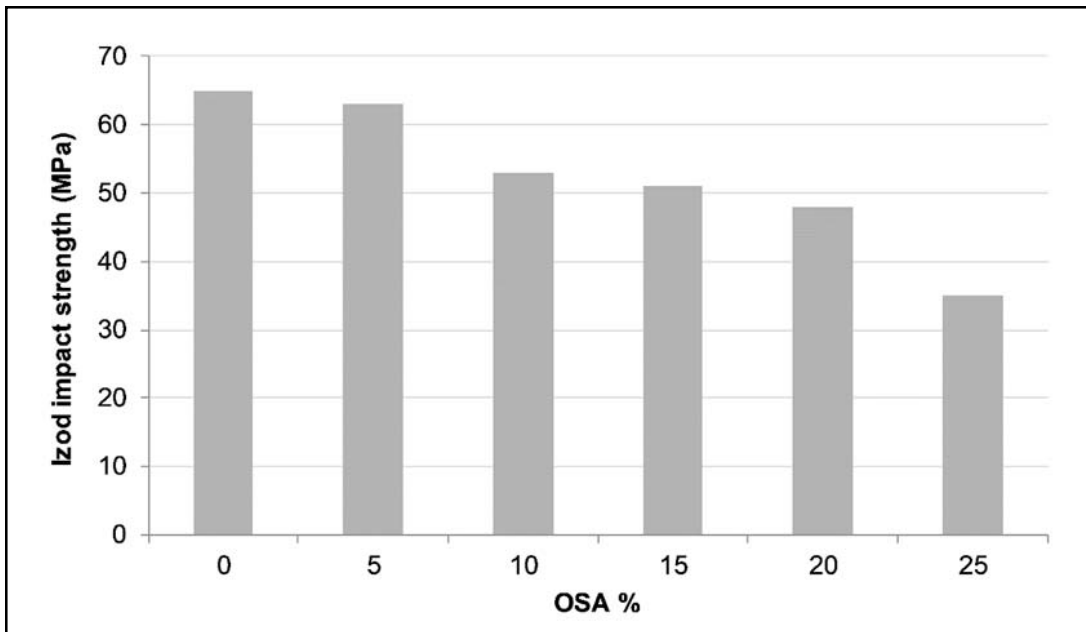

Figure 9. Effect of the OSA loading on the impact strength of the OSA-HDPE composite.

and modulus values increased with the increase in the filler content. The synergetic effect of the filler addition on the flexural strength and modulus may attributed to the limited number of voids, the small voids size, and the lack of agglomeration of the filler particles. The dispersed particles would absorb the applied energy and delay the crack propagation in the polymer composite as well.

3.1.4. Izod Impact Strength (un-notched)

In general, the amount of energy required to crack material is known as impact strength. Factors such as filler and matrix strength, bonding strength, filler distribution, and geometry are known to affect the impact strength of the composite materials. **Figure 9** represented the impact strength values of the OSA-HDPE polymer composite. The un-notched impact strength of the OSA-HDPE composite samples decreased as the filler content increased. It was observed that the addition of the OSA content up to 25%

decreased the impact strength of the composite by 46% compared to the pure HDPE polymer. Similarly, both absorbed energy and toughness were also decreased.

OSA particles decreased the elasticity of the polymer matrix which may accompanied with easy crack initiation of the composite. Similar behavior was found by Zhi Cao et al.[35] when peat ash was added to HDPE composites.

3.2 Water Absorption

In general composites based on the mineral fillers are less sensitive to humidity compared to that of cellulosic origin. The mechanical performance of the ash filled polymer composites were slightly affected by the water environment. The OSA Filler with good interfacial adhesion to polymer matrix improved some mechanical characters and reduced others as well. Water uptake % variation with the contact time at various filler loading levels is shown in **Figure 10**. Water uptake % rapidly
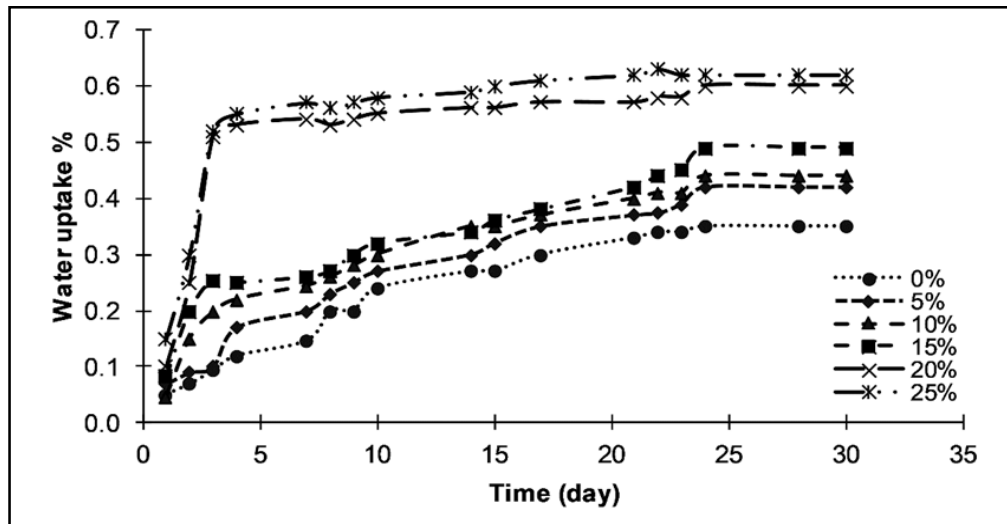

Figure 10. Water absorption of the OSA-HDPE composite vs. Time

increased in the first three days then slightly and gradually increased up to 25 days' immersion in water, after which no further water absorption observed with time. Composite samples with 20% and 25% filler contents showed higher water absorption values compared to composites with filler contents less than 15%. It was clear that the increase in the OSA filler content resulted in a slight increase in water absorption. Which was probably attributed to the filler that may increased the voids availability and allowed more space for the water molecules absorption, yet low water uptake % was observed.

3.3 Fractured Surface Morphology

SEM micrographs shown that the OSA filler has surface roughness and little irregular particle shape morphology with a particle size under 65 μm **Figure 11**.

Fractured surfaces of the pure HDPE and the OSA filled HDPE composites were also examined with SEM. Micrographs related to the fractured surface of the neat HDPE with 700x and 6200x magnifications have homogeneous surface with well-defined morphologies **Figure 12**.
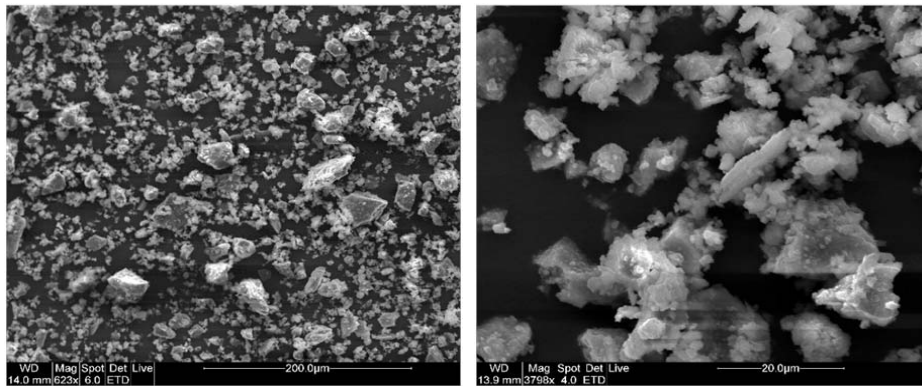

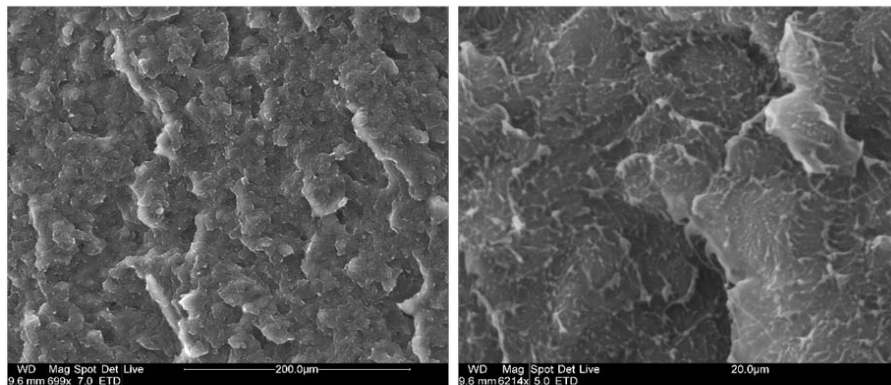
Figure 11. SEM micrographs of the OSA filler.

Figure 12. SEM micrographs of the fractured surface specimens of the neat HDPE at different magnifications.

Filler-matrix interfacial adhesion and surface area are important factors for reinforcing purposes. The filler dispersion with various loading levels was studied and shown in **Figure 13**. Composite phase boundaries are clearly shown between the OSA and the HDPE matrix. Where the OSA filler particulates were homogeneously dispersed within the polymer matrix. Filler size, shape, and loading levels parameters are crucial in determining the mechanical performance of the polymer composite materials.
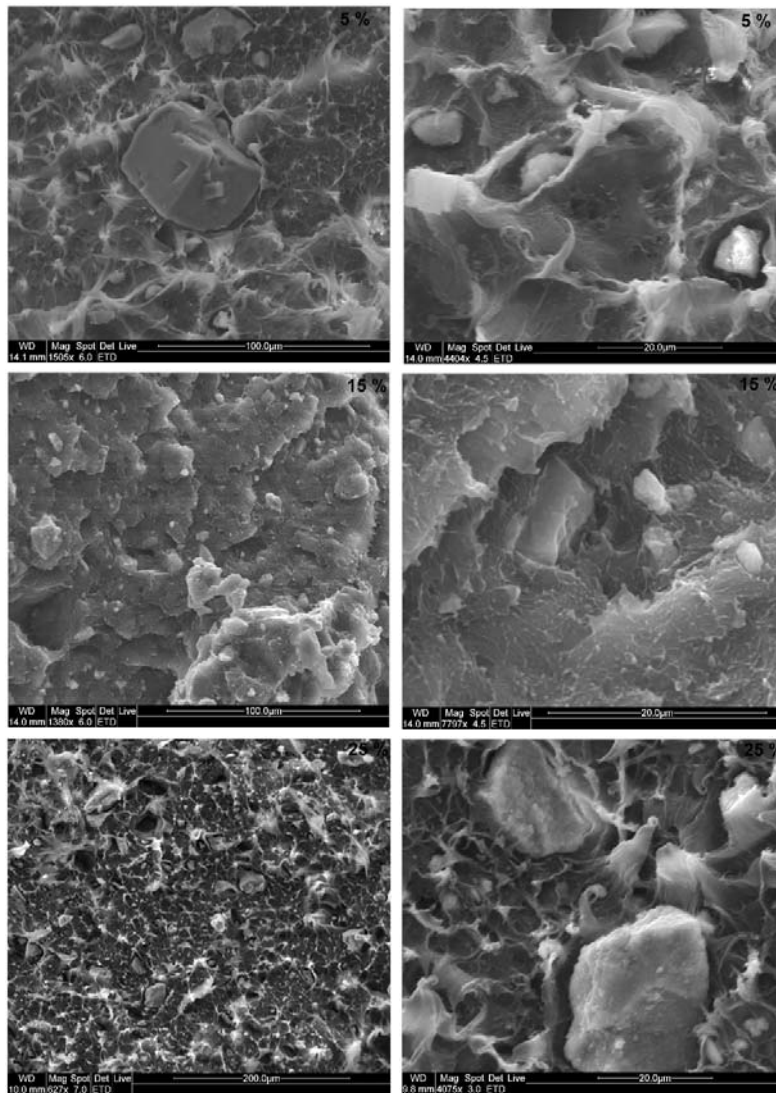

Figure 13. SEM micrographs of the fractured specimens of 5, 15 and 25 % OSA-HDPE composite.

Although SEM micrograph of the impact fractured surface showed no filler agglomeration yet the OSA filler particles still acted as a stress concentrator. As a result, the impact strength reduction was in direct proportion to the increase in the filler content as shown earlier in **Figure 9**. In general, while some fillers tend to decrease the impact resistance others can improve it especially for the brittle polymer. It was observed that 5–25 wt. % of the OSA reduced the impact resistance of the polymer composite. This was probably due to less cavitation on the surface of the polymer matrix upon impact which limited the impact energy distribution over a greater volume of the polymer matrix. More over the tensile strain at break followed the same behavior as impact strength. Less cavitation means less OSA particles debond, which is reasonably encouraged by the good interaction between the filler and the polymer matrix. Polymer composite cavitation behavior was in good agreement with the reduction in the strain at rapture and the impact strength data illustrated earlier in the stress-strain mechanical behavior section. The OSA filler with rough surface area was surrounded and adhered well with the HDPE polymer matrix. As a result, the stress at yield and rapture, flexural strength and modulus, and elastic modulus values had increased compared to those of the neat polymer.

4. CONCLUSION

OSA-HDPE composite, tensile stress at yield remained relatively unchanged up to 20 % wt. OSA and decreased by 10 % for 25% wt. OSA compared to the neat HDPE. Whereas the tensile strain at yield (43%) showed an increase when the OSA content was low up to 10%, after which a decline in the mean value (27%) was reported. The mean tensile stress at rapture (33 MPa) increased with the filler content. On the contrary, the tensile strain at rapture (40 %) showed a decrease in values as the filler loading level increased. Modulus of elasticity; a measure of material stiffness showed an increase (350 MPa) in stiffness with increasing the OSA filler content. Flexural strength of 22 MPa and modulus of 2.4 GPa showed an improvement in character with increasing the filler loadings. On the other hand, Impact strength of 50 MPa of the OSA-HDPE composite decreased with the filler loading. OSA-HDPE phase compatibility is good enough to balance various properties with acceptable mechanical performance. Water uptake percentages (0.5 %) increased as the OSA filler content increased yet values still marginal and did not significantly affect the composite shape and hardness even after 30 days of immersion in water.

Morphological microstructure illustrated the filler dispersion with no agglomerations and even less cavitation in the polymer matrix, all of which are in good agreement with the mechanical performance of the polymer composite.

Future research work related to the OSA filler loading level above 25 % with certain surface modification is promising in engineering new products with predetermined physical properties and targeted performance.

Conflicts of Interest

The authors declare that they have no conflicts of interest.

References

1. T. F. Yen and G. V. Chilingar, "Introduction to oil shales." In Developments in Petroleum Science, Elsevier, (1976): p.1.

2. Z. S. H. Abu-Hamatteh and A. F. Al-Shawabkeh, *Cen. Euro. Geol.* 51 (2008): 379.

3. K. Brendow, *Oil Shale*, 26 (2009): 357.

4. I. Külaots, J. L. Goldfarb and E. M. Suuberg, *Fuel*, 89 (2010): 3300.

5. O. Gavrilova, R. Vilu and L. Vallner, *Resour. Conserv. and Recy.* 55 (2010): 232.

6. I. Blinova, L. Bityukova, K. Kasemets, A. Ivask, A. Käkinen, I. Kurvet and H. Schvede, *J. Hazard. Mater.* 229 (2012): 192.

7. R. Anto, and JM. Punning. *Energy Environ. Sci.* 2 (2009) 723.

8. Z. Zhang, L. Zhang and A. Li, *J. Waste Manag.* 46 (2015): 316.

9. J. G. Jablonshi, Eighth International Ash Utilization Symposium. 2 (1978): 1.

10. M. O. Azzam and Z. Al-Ghazawi, *Constr. Build. Mater.* 101(2015): 359.

11. W. Wang, Y. Cheng, G. Tan and C. Shi, *Road Mater. Pavement.* 21(2020): 179.

12. H. Wei, Y. Zhang, J. Cui, L. Han and Z. Li, *Constr. Build Mater.* 196(2019): 204.

13. X. Guo, X. Chen, Y. Li, Z. Li and W. Guo, *Sustainability*. 11(2019): 4857.

14. M. O. Azzam, Z. Al-Ghazawi and A. Al-Otoom,*J.Clean. Prod.* 112(2019): 2259.

15. M. F. Attom, M. Smadi and T. Khedaywi, *Soils found.* 38(1998): 67.

16. A. Malik and A. Thapliyal, *Crit. Rev. Environ. Sci. Technol.* 39 (2009): 333.

17. A. Viikna, A. Krumme, A. Reinok, R. Kuusik and T. Kaljuvee, *W.O. Pat.* (2012): 2012083972A1.

18. I. Viira, *W.O. Pat.* (2018): 2017182043.

19. X. Huang, J. Y. Hwang and J. M. Gillis, *J. Miner. Mater. Charact. Eng.* 2(2003): 11.

20. C. Plowmanand N. B. Shaw, In AshTech'84-Conference Proceedings, London, (1984): p. 663.

21. S. S. Chuang, *U.S. Pat.* (2018): 9920179B2

22. H. Raymond T., L. Russell, Hill and J. Cornelius Bruce J. *U.S. Pat.* (2005): 6916863B2.

23. S. Nigel Peter, P. A. Shepheard and P. Michael, *U.S. Pat.* (2014): 20140306369A1.

24. I. Viira and K. Tiiu, *W. O. Pat.* (2011): 2011098091A1

25. R. Xianjie and E. Sancaktar. *J. clean. Prod.* 206 (2019): 374

26. Y. H. Liu, X. X. Xue and J. M. Shen, *FDMP*, 11(2015): 197.

27. L. K. Roger L. *Plast Design Process*, 18(1978): 49.

28. Sim J, Kang Y, Kim BJ, Park YH, Lee YC. Polymers. 12(2020): 79.

29. MM. Smadi and RH. Haddad, *Cem. Concr. Compos.* 25(2003): 43.

30. RH. Haddad, AM. Ashtey at and ZK. Lababneh, *Struct. Concr.* 20 (2019): 225.

31. P. Peeter, P. Paiste, M. Liira and K. Kirsimäe, *Oil Shale,* 36 (2019): 14.

32. MC. Usta, CR. Yörük, T. Hain, P. Paaver, R. Snellings, E Rozov, A. Gregor, R. Kuusik, A. Trikkel and M. Uibu. *Minerals*, 10 (2020): 765.

33. YW. Leong, MB. Abu Bakar, ZM. Ishak, A. Ariffin and B. Pukanszky. *J. Appl. Polym. Sci.* 91 (2004): 3315.

34. B. Pukanszky, E. Fekete and F. Tudos. *Makromol. Chem. Macromol. Symp.* 28(1989): 165.

35. Z. Cao, M. Daly, LM. Geever, I. Major, CL. Higginbotham and DM. Devine. *Compos. B Eng.* 94(2016): 312.